BUTTERWORTH HEINEMANN

Polymer Vol. 36 No. 23, pp. 4433–4438, 1995

0032-3861/95/$10.00+0.00

Photon diffusion study in films formed from high-T latex particles

Murat Canpolat and Onder Pekcan*
Department of Physics, Istanbul Technical University, 80626, Maslak, Istanbul, Turkey
(Received 15 May 1994; revised 28 September 1994)

The steady-state fluorescence technique was used to study the evolution of transparency during film formation from high-T latex particles. The latex films were prepared from pyrene-labelled poly(methyl methacrylate) particles and annealed in 10 min time intervals above the glass transition temperature (T_g). Scanning electron microscopy was used to detect the variation in physical structure of annealed films. Monte Carlo simulations were performed for photons diffusing the latex films and the number of emitted and scattered photons was calculated. The crossing density of polymer chains at the particle–particle interface was found to depend linearly on $(\text{time})^{1/2}$. The activation energy for back-and-forth motion of a reptating polymer chain was measured and found to be 29 kcal mol^{-1}. The corresponding frequencies of a reptating chain were between 1.5 and 42 s^{-1} above T_g.

(Keywords: latex films; photon diffusion; activation energy)

INTRODUCTION

Aqueous or non-aqueous dispersions of colloidal particles with glass transition temperature (T_g) above the drying temperature are generally named high-T latex dispersions, while aqueous dispersions of colloidal particles with T_g below the drying temperature are called low-T latex dispersions. The term 'latex film' normally refers to a film formed from low-T particles where the forces accompanying the evaporation of water are sufficient to compress and deform the particles into a transparent, void-free film[1,2]. However, high-T latex particles remain essentially discrete and undeformed during the drying process. Latex films can also be obtained by compression moulding of a dried latex powder composed of polymers such as polystyrene (PS) or poly(methyl methacrylate) (PMMA) which have T_g above room temperature.

The mechanical properties of high-T films can be evolved by annealing after all solvent has evaporated. This process, called sintering, is an important aspect of latex coatings and represents an important feature that it is desirable to understand. The mechanism of film formation by annealing of high-T latex films is known as interdiffusion of polymer chains and is followed by healing at the particle–particle interface. In general, when two identical polymeric materials are brought into intimate contact and heated at a temperature above T_g, the polymer chains become mobile and interdiffusion of polymer chains across the interface can occur. After this process, the junction surface becomes indistinguishable in all respects from any other surface that might be located in the polymeric material. This process is called 'healing of the junction' by which the joint achieves the same cohesive strength as the bulk polymeric material.

* To whom correspondence should be addressed

The word 'interdiffusion' in polymer science is used for the process of mixing, intermingling and homogenization at the molecular level, which implies diffusion among polymer chains.

In the bulk state, polymer chains have a Gaussian distribution of segments. Chains confined to the half-space adjacent to the junction have distorted conformations[3–5]. Diffusion across the junction leads to configurational relaxation and recovery of Gaussian chain behaviour. Polymers much larger than a certain length are often pictured as confined to a tube, and diffusion occurs by a reptile-like motion. In this model, each polymer chain is considered to be confined to a tube along the length of which it executes a random back-and-forth motion. This reptile-like motion will cause the chain to slip out of a section of tube at one end or the other. The reptation time (T_R) describes the time necessary for a polymer to diffuse a sufficient distance for all memory of the initial tube to be lost. This is the time it takes for initial configuration to be forgotten and the first relaxation to be completed.

Transmission electron microscopy (TEM) is the most common technique used to investigate the structure of dried films[6,7]. A pattern of hexagons, consistent with face-centred cubic packing, is usually observed in highly ordered films. When these films are annealed, complete disappearance of structure is sometimes observed, which is consistent with extensive polymer interdiffusion. Freeze-fracture TEM has been used to study the structure of dried latex films[8,9]. Small-angle neutron scattering (SANS) has been used to study latex film formation at the molecular level. Extensive studies using SANS have been performed by Sperling and co-workers[10] on compression-moulded PS film. Direct non-radiative energy transfer has been employed to investigate the film formation processes from dye-labelled high-T[11] and low-T[12,13] polymeric particles.

The steady-state fluorescence (SSF) technique combined with DET was recently used to examine healing the interdiffusion processes in dye-labelled high-T latex systems[14–18]. In the SSF technique the quality of film is more critical than in time-resolved fluorescence measurements[11,12]. Because of photon diffusion, special attention has to be paid to studying the evolution of transparency of the latex film during SSF measurement.

In this work we studied the evolution of transparency of films formed from high-T latex particles, by monitoring the intensities of excited light (I_{sc}) and of fluorescence emission (I_{op}) from a dye, using the SSF technique. It was shown that the variation in transparency is related to the variation in I_{op}. Isothermal experiments were performed by annealing latex films in equal time intervals and direct fluorescence emission was monitored to study chain flow across the particle–particle junction. An increase in dye intensity by increasing the number of annealing time intervals was attributed to an increase in the 'crossing density' at the junction surface. The method developed by Prager and Tirrell (PT)[4] was employed to investigate the healing processes at the junction.

In the SSF experiments, the high-T latex particles used were labelled with pyrene (P) dye and had two components[19,20]: the major part, PMMA, comprised 96 mol% of the material and the minor component, polyisobutylene (PIB) (4 mol%), formed an interpenetrating network through the particle interior[21,22] which was very soluble in certain hydrocarbon media. A thin layer of PIB covered the particle surface and provided colloidal stability by steric stabilization.

In this paper, Monte Carlo simulations were performed to calculate the scattered and emitted photon intensities from a film by using photon diffusion theory (PDT)[23]. Evolution of transparency is modelled by the variation in mean-free path of a photon in latex films at each annealing step. The increase in optical path of a photon is explained by the healing processes.

EXPERIMENTAL

Pyrene (P)-labelled PMMA–PIB polymer particles were prepared separately in a two-step process; in the first step MMA was polymerized to low conversion in cyclohexane in the presence of PIB containing 2% isoprene units to promote grafting. The graft copolymer so produced served as a dispersant in the second stage of polymerization, in which MMA was polymerized in a cyclohexane solution of the polymer. Details of the process have been published[19]. A stable dispersion of spherical polymer particles was produced, with radius ranges from 1 to 3 μm. A combination of ^{1}H nuclear magnetic resonance (n.m.r.) and u.v. analysis indicated that these particles contained 6 mol% PIB and 0.037 mmol P groups per gram of polymer. Latex film preparation was carried out by dispersing particles in heptane in a test tube with the solid content taken to be 1%.

In this work, SSF experiments were carried out with isothermally annealed latex film samples. Films with 3.5 layers were prepared from the dispersion of particles by placing different numbers of drops on round silica window plates with a diameter of 1.35 cm and allowing the heptane to evaporate. Care was taken to ensure that the liquid dispersion from droplets covered the whole surface area of the plates and remained there until the heptane had evaporated. Samples were weighed before and after film casting to determine the film thicknesses. The average size of particles was taken to be 2 μm in order to calculate the number of layers of the films.

Latex film samples were isothermally annealed above the T_g of PMMA for 10 min time intervals at 150, 160, 170, 180 and 190°C. The temperature was maintained to within ±2 °C during annealing. After annealing, each sample was placed in the solid surface accessory of a fluorescence spectrometer (Perkin–Elmer model LS-50). P was excited at 345 nm and fluorescence emission was detected between 370 and 440 nm. All measurements were carried out in the front-face position at room temperature. Slit widths were kept at 2.5 mm during all SSF measurements.

Samples cast from a chloroform solution of particles were used as a model for the fully transparent films.

For scanning electron microscopy (SEM), a Hummer VII sputtering system was used for gold-coating, and films of particles were then examined at 10–15 kV in a JEOL JSM-T330 microscope.

PHOTON DIFFUSION IN LATEX FILMS

The journey of an exciting or emitted photon to or from a dye molecule in a film formed from annealed latex particles can be modelled by photon diffusion theory[23]. The collision probability, P, of a travelling photon with any scattering centre in a film is given by:

$$P = 1 - \exp(-r/ < r >) \quad (1)$$

where r is the distance travelled by a photon between consecutive collisions and $< r >$ is defined as the mean-free path of a photon. Here, the film is taken as a plane sheet with thickness d, and the direction of incident photons is taken to be perpendicular to the film surface (for example, in the z direction). In Monte Carlo simulations, after each collision, d is compared with the z component of the total distance:

$$s_z = \sum_i^n r_{iz}$$

where i is the number of successive collisions during the journey of a photon. Photons emerging from the back and front surfaces without interacting with a pyrene molecule of the film then have to satisfy the conditions:

$$s_z > 0 \text{ and } s_z < 0 \quad (2)$$

respectively. The total number of photons emerging from the front surface is then represented by N_{sc}, which is assumed to model the intensity, I_{sc}, of light scattered from the latex film during SSF measurements.

In order to model the relation for the fluorescence intensity, I_{op}, emitted from the latex film, we defined the probability of a photon encountering a pyrene molecule to be:

$$q = 1 - \exp(-s/l) \quad (3)$$

where s represents the total distance travelled by the photon in the film (optical path) and l is the mean distance the photon travels in the film before it finds a pyrene molecule. If s is large, the probability of the photon encountering a pyrene molecule is high, and *vice versa*. After collision with a pyrene molecule, the photon

travels again according to equation (1). Then d is compared with the z component of the total distance, s_z, as in equation (2), to find the number of photons emitted from the film surfaces. The number of photons emitted from the front surface of the film is given by N_{op}, which is assumed to model the fluorescence intensity, I_{op}, emitted from the latex film.

In Monte Carlo simulations, l and d are taken to be fixed parameters with values of 10 and 180, respectively. It should be noted that l is considered to be proportional to pyrene concentration in the latex film, which is constant during the film formation processes, and time, t, is taken to be proportional to $< r >$. The mean-free path, $< r >$, was varied between 1 and 20 for a given d and for each $< r >$ the incident number of photons was taken to be 3×10^4 during the simulations. The number of collisions, n, is varied so that the conditions in equation (2) are satisfied.

RESULTS AND DISCUSSION

Transparency of films and optical path of photons

Typical emission (I_{op}) and scattered (I_{sc}) spectra of a 3.5-layer latex film annealed at 180°C for 10 min time intervals and excited at 345 nm are shown in *Figure 1*. In this sample I_{op} increased while I_{sc} decreased continuously with increasing number of annealing time intervals. I_{op} and I_{sc} *versus* annealing time are plotted in *Figures 2a* and *b*, respectively, for the sample presented in *Figure 1*. The last points in *Figures 2a* and *b* represent I_{op} and I_{sc} of a film cast from a chloroform solution of latex particles. In order to interpret these behaviours of I_{op} and I_{sc}, their models (N_{op} and N_{sc}) from Monte Carlo simulations are plotted against mean-free path $< r >$ of a photon in *Figures 3a* and *b*, respectively. The similarities between *Figures 2* and *3* should be noted, from which it is suggested that, as the annealing time increases, $< r >$ of a photon increases due to the disappearance of voids between particles in the latex film at an early stage of annealing during which both I_{op} and N_{op} start to increase. Later, however, both I_{op} and N_{op} become saturated with increasing time and $< r >$, respectively, indicating that the healing process at the particle–particle junction[16,17] becomes effective.

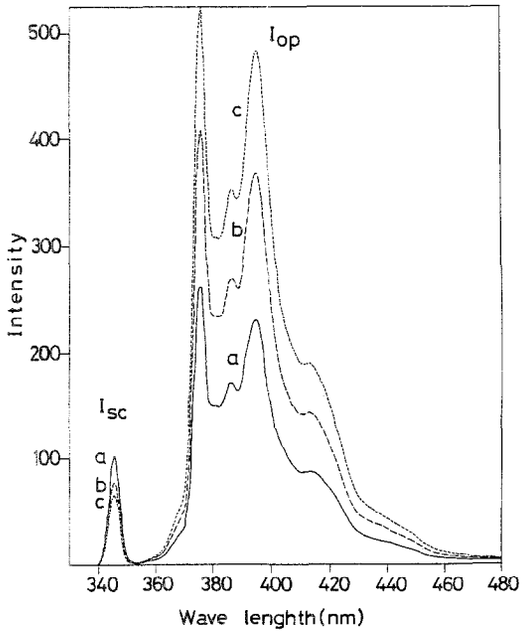

Figure 1 Emission (I_{op}) and scattered (I_{sc}) spectra of a 3.5-layer latex film after annealing at 180°C for (a) 10 min, (b) 3×10 min, (c) 7×10 min time intervals

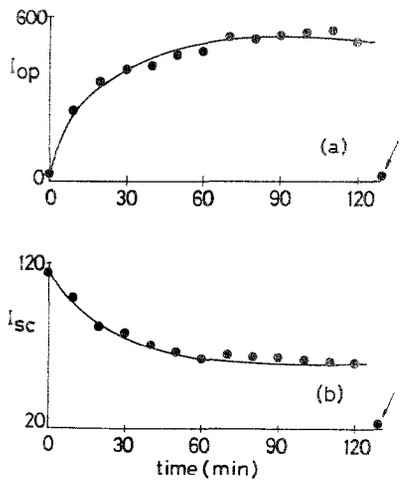

Figure 2 Plot of (a) I_{op} and (b) I_{sc} *versus* annealing time for a 3.5-layer film sample. The sample is excited at 345 nm and annealed at 10 min time intervals. The last points in the plots, indicated by arrows, belong to the chloroform-cast film

The variation in I_{op} and N_{op} depends on the mean optical path, s, of a photon in the film. This mean optical path is directly proportional to the probability of the photon encountering a pyrene molecule. At the very early stage of annealing, the photon is scattered from the particle surfaces, the mean-free path, $< r >$, is of the order of the size of the interparticle voids, and after a few steps it re-emerges from the front surface of the film. Thus, the mean optical path, s, is very short, which give rise to high I_{sc} (and N_{sc}) and low I_{op} (and N_{op}) values. As the healing process proceeds, the scattering is predominantly from the interparticle interfaces and the mean-free path becomes of the order of the particle size. Clearly, in this stage, with the same number of photons rescattering, a photon will spend a much longer time in the film, and

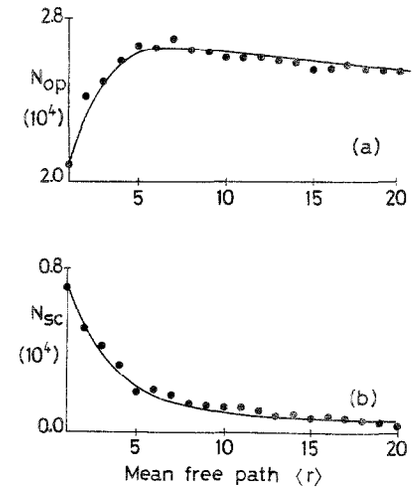

Figure 3 Variation in number of photons (a) emitted N_{op} and (b) scattered N_{sc} from the front surface of a film with respect to mean-free path $< r >$ of a photon. The number of incident photons for each $< r >$ is taken as 3×10^4 during Monte Carlo simulations

consequently I_{op} (and N_{op}) increase, while I_{sc} (and N_{sc}) decrease. The slight decrease in N_{op} at high $< r >$ values in *Figure 3a* can be interpreted by the escape of some photons from the back surface of the film. Naturally, as $< r >$ increases, photons can reach the back surface easily and N_{op} decreases. For chloroform-treated samples, I_{op} showed a very low value compared to annealed latex films. This observation can be explained by the large $< r >$ and small s values in the fully transparent film, in which the probability of a photon encountering a pyrene molecule is quite low. A low I_{sc} value is also expected from this highly transparent film, which was shown in *Figure 2b*.

In order to support these findings, scanning electron micrographs of latex films, before and after annealing at 160°C and 180°C for 30 min, are presented in *Figure 4* together with the chloroform-treated sample. In *Figure 4a*, individual latex particles can be seen in a powder film containing many voids. However, in *Figures 4b* and *c*, SEM images show the disappearance of particle boundaries due to annealing of latex films for 30 min total time at 160°C and 180°C, respectively. The films in *Figure 4b* and *c* have higher I_{op} values than the film in *Figure 4a*, indicating that photons have longer $< r >$ and s values in the former samples, where refraction can occur many times between particle interfaces. Finally, chloroform-treated film in *Figure 4d* shows no trace of particles, suggesting high $< r >$ and low s values, which cause very low I_{op} and I_{sc} values.

SEM results together with Monte Carlo simulations support SSF observations in *Figure 2*. A diagram of film formation from high-T latex particles and its relation to the mean-free and optical paths ($< r >$ and s) is presented in *Figure 5* to further illustrate our findings. *Figure 5a* presents the early stage of film formation, where heptane evaporates and close-packed particles form a powder film, which includes many voids. In this film, $< r >$ and s values are quite low and a photon is emitted immediately from the front surface of the film, which should have low I_{op} and high I_{sc} values. *Figure 5b* represents a film where, due to annealing, particle boundaries start to heal and disappear, and as a result the incident photon has a longer $< r >$ value. In this case, a photon can be refracted many times in the film and has a higher probability of finding a pyrene molecule. This film should have high I_{op} and low I_{sc} values. A diagram of the chloroform-treated film is shown in *Figure 5c*, with the longest $< r >$ but shorter s values.

Crossing density of junction surface

When film samples with 3.5 layers were annealed at 150, 160, 170, 180 and 190°C, for 10 min time intervals, a continuous increase in I_{op} was observed until they were saturated. The increase in I_{op} was explained in the previous section as due to the increase in transparency of latex film due to the disappearance of voids at the early stage of annealing. Later, as the annealing time is increased, part of the polymer chains may cross the junction surface and particle boundaries start to disappear. At this stage the optical path becomes longer and as a result the emission intensity I_{op} increases until it is saturated.

In order to interpret these results, the PT model[4] for chain-crossing density was employed. These authors used de Gennes' 'reptation' model[3] to explain configurational

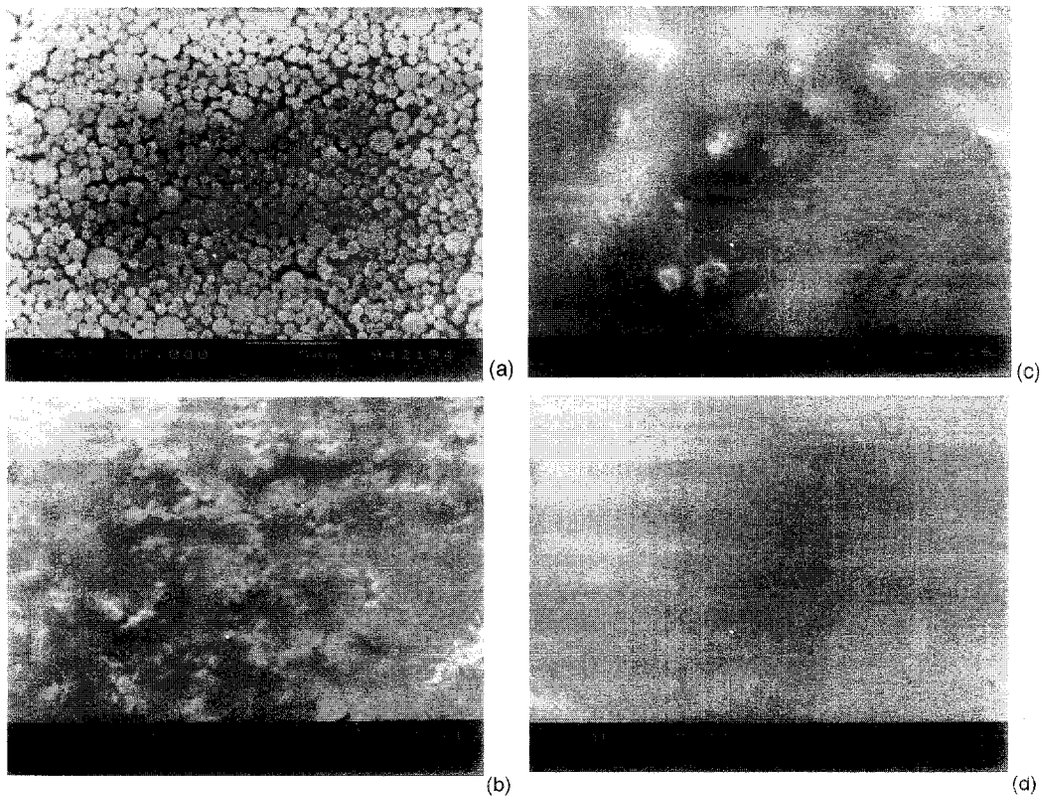

Figure 4 Scanning electron micrographs of latex film samples: (a) before annealing, (b) annealed at 160°C for 3 × 10 min, (c) annealed at 180°C for 3 × 10 min, (d) chloroform-treated film

relaxation at the polymer–polymer junction, where each polymer chain is considered to be confined to a tube in which it executes a random back-and-forth motion. A homopolymer chain with N freely jointed segments of length L was considered by PT, which moves back and forth by one segment with a frequency ν. In time, the chain displaces down the tube by a number of segments, m. Here, $\nu/2$ is called the 'diffusion coefficient' of m in one-dimensional motion. PT calculated the probability of the net displacement with m during time t in the range of $n-\Delta$ to $n-(\Delta+\mathrm{d}\Delta)$ segments. A Gaussian probability density was obtained for small times and large N. The total 'crossing density' $\sigma(t)$ (chains per unit area) at the junction surface was then calculated from the contributions $\sigma_1(t)$ due to chains still retaining some portion of their initial tubes, plus a remainder, $\sigma_2(t)$. Here, the $\sigma_2(t)$ contribution comes from chains which have relaxed at least once. In terms of reduced time, $\tau = 2\nu t/N^2$, the total crossing density can be written as:

$$\sigma(\tau)/\sigma(\infty) = 2\pi^{-1/2}\{\tau^{1/2} + 2\sum_{k=0}^{\infty}(-1)^n \times [\tau^{1/2}\exp(-k^2/\tau) - \pi^{-1/2}\mathrm{erfc}(k/\tau^{1/2})]\} \quad (4)$$

For smaller τ values the summation term of equation (4) is very small and can be neglected, which then results in:

$$\sigma(\tau)/\sigma(\infty) = 2\pi^{-1/2}\tau^{1/2} \quad (5)$$

This was predicted by de Gennes on the basis of scaling arguments[3]. In order to compare our results with the crossing density of the PT model, I_{op} values are plotted against $t^{1/2}$ in *Figure 6* for films annealed at 160, 170 and 180°C. I_{op} increases linearly for all samples. As pointed out before, the increase in I_{op} can be related to the disappearance of particle–particle boundaries. As annealing time increases, more chains relax across the junction surface and as a result the crossing density increases. Here, we assume that I_{op} is directly proportional to the crossing density $\sigma(t)$ during film formation processes. The linear behaviour of I_{op} *versus* $t^{1/2}$ might be related to the $\sigma_1(t)$ term in the PT model, which is inherited from the chains still retaining a portion of their initial tube. *Figure 7* shows a diagram of the contribution of $\sigma_1(t)$ and $\sigma_2(t)$ terms to the healing process at the particle–particle junction. Experimental results in *Figure 6* are consistent with the PT theoretical predictions in equation (5).

The temperature dependence of I_{op}, which is assumed to be proportional to $\sigma(\tau)/\sigma(\infty)$, can be quantified by using equation (5), where the Arrhenius relation for the linear diffusion coefficient is used as:

$$\nu = \nu_0\exp(-\Delta E_b/kT) \quad (6)$$

where ΔE_b is defined as the activation energy for the back-and-forth motion. According to equation (6), for low temperatures, $\sigma(\tau)$ varies slowly with time as shown in *Figure 6a*. When the annealing temperature is increased, then more chains can be relaxed across the junction surface and I_{op} varies faster with time, as presented in *Figure 6c*. ν values were estimated from the slopes of *Figures 6a, b* and *c* and were found to be 6.54, 8.86 and 12.18 s^{-1} for 160, 170 and 180°C, respectively. Here, equation (5) was used and the number of segments was taken as $N = 500$ to obtain the ν values. ν values for two different sets of experiments were obtained at various temperatures and are listed in *Table 1*. Here one may suggest that ν values are associated with the short-range back-and-forth motion of the polymer chain

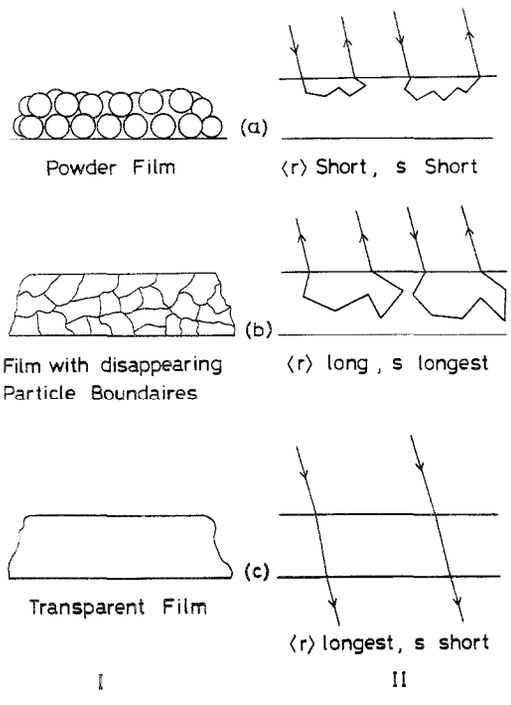

Figure 5 Diagram of (a) powder latex film, (b) film with disappearing particle boundaries, (c) chloroform-treated transparent film. $< r >$ and s represent mean-free and optical paths, respectively, travelled by a photon in the films

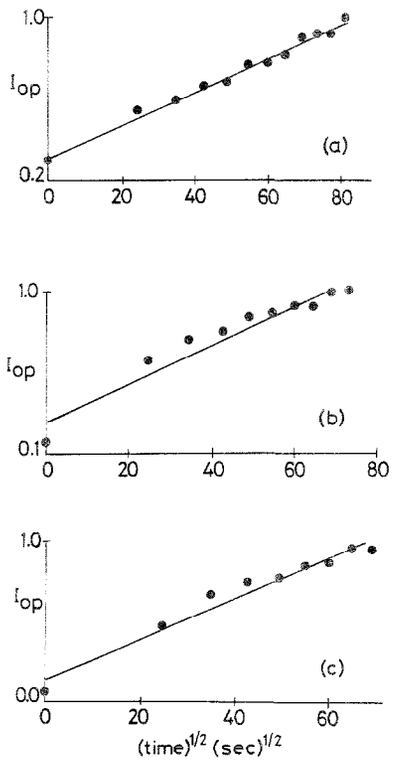

Figure 6 Plot of I_{op} *versus* $t^{1/2}$ for samples annealed at (a) 160°C, (b) 170°C and (c) 180°C in 10 min intervals

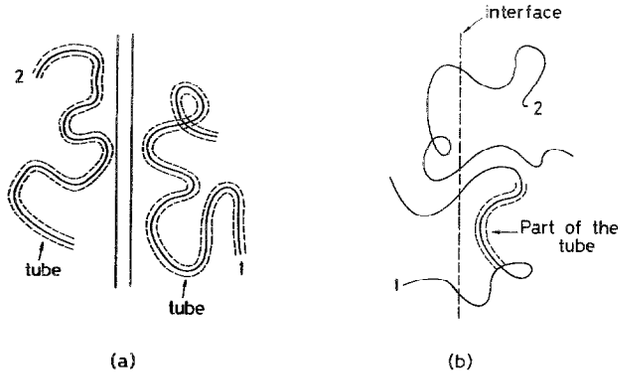

Figure 7 Diagram of chains at (a) particle–particle junction, (b) healed interface. 1 represents a chain still retaining the same portion in its initial tube and 2 represents a chain relaxed at least once

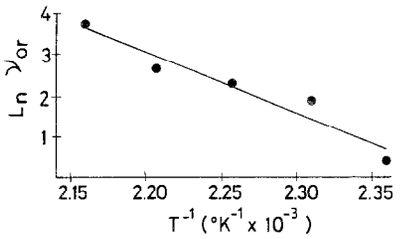

Figure 8 Logarithmic plot of ν_{or} values *versus* T^{-1} for the data obtained from experiments a and b in *Table 1*. Slopes were obtained by fitting the data to equation (6)

in the tube at the corresponding temperatures. When the inverse values of these characteristic frequencies are compared with the healing (τ_H) at the corresponding temperatures[16,17](from 30 to 5 min), it is found that the back-and-forth times ($\nu_{or}s^{-1}$) are 10^4 times smaller than τ_H times. These findings are quite reasonable from the point of view that a 'polymer chain executes many back-and-forth motions before it relaxes at least once'.

A logarithmic plot of ν_{or} values *versus* T^{-1} is presented in *Figure 8*. ΔE_b energy was produced by fitting the data in *Table 1* to equation (6) and was found to be 29.4 kcal mol^{-1}, which is quite large compared to the healing activation energy[15–17] ($\Delta E_H = 10$ kcal mol^{-1}). Since ΔH_H is responsible for the motion of a minor chain (segmental motion), it is reasonable to expect that the back-and-forth motion needs a higher activation energy in order to be executed. In conclusion, we have developed a novel method to measure the back-and-forth frequencies and the activation energy for a reptating chain at the particle–particle interface during annealing of high-T latex films. These experiments are easy to perform and the spectrometer is quite inexpensive to obtain.

Table 1 Experimentally obtained ν values from two different sets of experiments (a and b). Equations (5) and (6) were used to fit the I_{op} *versus* $t^{1/2}$ plots to obtain ν values. ν_{or} is found taking the average of ν values from experiments a and b

	Temperature (°C)					
	150	160	170	180	190	Experiment
ν (s^{-1})	1.51	6.54	8.86	12.18	41.58	a
ν (s^{-1})	1.41	6.52	11.14	15.81	41.99	b
ν_{or} (s^{-1})	1.46	6.53	9.99	13.99	41.78	–
ν_{or} (s^{-1})	0.68	0.15	0.10	0.071	0.024	–

ACKNOWLEDGEMENT

We thank Professor M. A. Winnik for supplying us with the material and supporting O. Pekcan during his stay in Toronto. Mr B. Williamson is thanked for preparing the polymer particles.

REFERENCES

1 Eckersley, S. T. and Rudin, A. *J Coatings Technol.* 1990, **62**(780), 89
2 Joanicot, M., Wong, K., Maquet, J., Chevalier, Y., Pichot, C., Graillat, C., Linder, P., Rios, L. and Cabane, B. *Prog. Colloid Polym. Sci.* 1990, **81,** 175
3 de Gennes, P. G. *C.R. Acad. Sci. (Paris)* 1980, **291,** 219
4 Prager, S. and Tirrell, M. *J. Chem. Phys.* 1981, **75,** 5194
5 Kim, Y. H. and Wool, R. P. *Macromolecules* 1983, **16,** 115
6 Vanderhoff, J. W. *Br. Polym. J.* 1970, **2,** 161
7 Kanig, G. and Neff, H. *Colloid Polym. Sci.* 1975, **256,** 1052
8 Wang, Y., Kats, A., Juhue, D., Winnik, M. A., Shivers, R. R. and Dinsdale, C. J. *Langmuir* 1992, **8,** 1435
9 Roulstone, B. J., Wilkinson, M. C., Hearn, J. and Wilson, A. J. *Polym. Int.* 1991, **24,** 87
10 Kim, K. D., Sperling, L. H. and Klein, A. *Macromolecules* 1993, **26,** 4624
11 Pekcan, O., Winnik, M. A. and Croucher, M. D. *Macromolecules* 1990, **23,** 2673
12 Wang, Y., Zhao, C. L. and Winnik, M. A. *J. Chem. Phys.* 1991, **95,** 2143
13 Wang, Y. and Winnik, M. A. *Macromolecules* 1993, **26,** 3147
14 Pekcan, O., Canpolat, M. and Göçmen, A. *Eur. Polym. J.* 1993 **29,** 115
15 Pekcan, O., Canpolat, M. and Göçmen, A. *Polymer* 1993, **34,** 3319
16 Canpolat, M. and Pekcan, O. *Polymer* 1995, **36,** 2025
17 Pekcan, O. *Trends Polym. Sci.* 1994, **2,** 236
18 Pekcan, O. and Canpolat, M. *Polym. Adv. Technol.* 1994, **5,** 479
19 Winnik, M. A., Hua, M. H., Hongham, B., Williamson, B. and Croucher, M. D. *Macromolecules* 1984, **17,** 262
20 Pekcan, O., Winnik, M. A. and Croucher, M. D. *Macromolecules* 1994 **17,** 262
21 Pekcan, O., Winnik, M. A. and Croucher, M. D. *Phys. Rev. Lett.* 1988, **61,** 641
22 Pekcan, O., *Chem. Phys. Lett.* 1992, **20,** 198
23 Meeten, G. H. 'Optical Properties of Polymers', Elsevier Science, New York, 1989